AGU PUBLICATIONS

Geophysical Research Letters

RESEARCH LETTER
10.1002/2017GL075571

Key Points:
- Permafrost stores a significant amount of mercury
- Permafrost regions store twice as much mercury as all other soils, the ocean, and atmosphere combined
- Thawing permafrost in a warming climate may release mercury to the environment

Supporting Information:
- Supporting Information S1
- Data Set S1
- Data Set S2

Correspondence to:
P. F. Schuster,
pschuste@usgs.gov

Citation:
Schuster, P. F., Schaefer, K. M., Aiken, G. R., Antweiler, R. C., Dewild, J. F., Gryziec, J. D., … Zhang, T. (2018). Permafrost stores a globally significant amount of mercury. *Geophysical Research Letters*, *45*, 1463–1471. https://doi.org/10.1002/2017GL075571

Received 27 SEP 2017
Accepted 10 JAN 2018
Published online 5 FEB 2018
Corrected 20 JUN 2018

This article was corrected on 20 JUN 2018. See the end of the full text for details.

Permafrost Stores a Globally Significant Amount of Mercury

Paul F. Schuster[1], Kevin M. Schaefer[2], George R. Aiken[1,3], Ronald C. Antweiler[1], John F. Dewild[4], Joshua D. Gryziec[5], Alessio Gusmeroli[6], Gustaf Hugelius[7], Elchin Jafarov[8], David P. Krabbenhoft[4], Lin Liu[9], Nicole Herman-Mercer[1], Cuicui Mu[10], David A. Roth[1], Tim Schaefer[11], Robert G. Striegl[1], Kimberly P. Wickland[1], and Tingjun Zhang[10]

[1]U.S. Geological Survey, National Research Program, Boulder, CO, USA, [2]National Snow and Ice Data Center, Cooperative Institute for Research in Environmental Sciences, University of Colorado Boulder, Boulder, CO, USA, [3]Deceased, [4]U.S. Geological Survey, Wisconsin Water Science Center, Mercury Research Laboratory, Middleton, WI, USA, [5]Environmental Service Lab, Broomfield, CO, USA, [6]International Arctic Research Center, University of Alaska, Fairbanks, AK, USA, [7]Department of Physical Geography, Stockholm University, Stockholm, Sweden, [8]Computational Earth Sciences, Los Alamos National Laboratory, Los Alamos, NM, USA, [9]Earth System Science Programme, Faculty of Science, Chinese University of Hong Kong, Hong Kong, [10]Key Laboratory of Western China's Environmental Systems (MOE), College of Earth and Environmental Sciences, Lanzhou University, Lanzhou, China, [11]Galmont Consulting, Chicago, IL, USA

Abstract Changing climate in northern regions is causing permafrost to thaw with major implications for the global mercury (Hg) cycle. We estimated Hg in permafrost regions based on in situ measurements of sediment total mercury (STHg), soil organic carbon (SOC), and the Hg to carbon ratio (R_{HgC}) combined with maps of soil carbon. We measured a median STHg of 43 ± 30 ng Hg g soil^{-1} and a median R_{HgC} of 1.6 ± 0.9 μg Hg g C^{-1}, consistent with published results of STHg for tundra soils and 11,000 measurements from 4,926 temperate, nonpermafrost sites in North America and Eurasia. We estimate that the Northern Hemisphere permafrost regions contain 1,656 ± 962 Gg Hg, of which 793 ± 461 Gg Hg is frozen in permafrost. Permafrost soils store nearly twice as much Hg as all other soils, the ocean, and the atmosphere combined, and this Hg is vulnerable to release as permafrost thaws over the next century. Existing estimates greatly underestimate Hg in permafrost soils, indicating a need to reevaluate the role of the Arctic regions in the global Hg cycle.

Plain Language Summary Researchers estimate the amount of natural mercury stored in perennially frozen soils (permafrost) in the Northern Hemisphere. Permafrost regions contain twice as much mercury as the rest of all soils, the atmosphere, and ocean combined.

1. Introduction

Over thousands of years, sedimentation buried mercury (Hg) bound to organic material and froze it into the permafrost (Obrist et al., 2017). Permafrost is soil at or below 0°C for at least two consecutive years. The active layer is the surface soil layer on top of the permafrost that thaws in summer and refreezes in winter (Figure S1 in the supporting information). Hg deposits onto the soil surface from the atmosphere, where it bonds with organic matter in the active layer. Microbial decay then consumes the organic matter, releasing the Hg (Smith-Downey et al., 2010). At the same time, sedimentation slowly increases soil depth such that organic matter at the bottom of the active layer becomes frozen into permafrost. The organic matter consists almost entirely of plant roots, and, once frozen, microbial decay effectively ceases, locking the Hg into the permafrost. However, permafrost has begun to thaw under a changing climate (Hinzman et al., 2005; Romanovsky et al., 2008; Smith et al., 2010). Once the permafrost and associated organic matter thaws, microbial decay will resume and release Hg to the environment, potentially impacting the Arctic Hg balance, aquatic resources, and human health (Dunlap et al., 2007; Jonsson et al., 2017; Obrist et al., 2017; USGS Fact Sheet, https://www2.usgs.gov/themes/factsheet/146-00/, 2016). Model projections estimate a 30–99% reduction in the area of Northern Hemisphere permafrost by 2100, assuming anthropogenic greenhouse gases emissions continue at current rates (Koven et al., 2013). In a novel approach, we make the first-ever estimate of the storage of Hg in the Northern Hemisphere permafrost soils using empirical relationships based on in situ measurements of sediment total mercury (STHg) combined with published maps of soil organic carbon (Hugelius, Tarnocai, et al., 2013; Hugelius, Bockheim, et al., 2013).

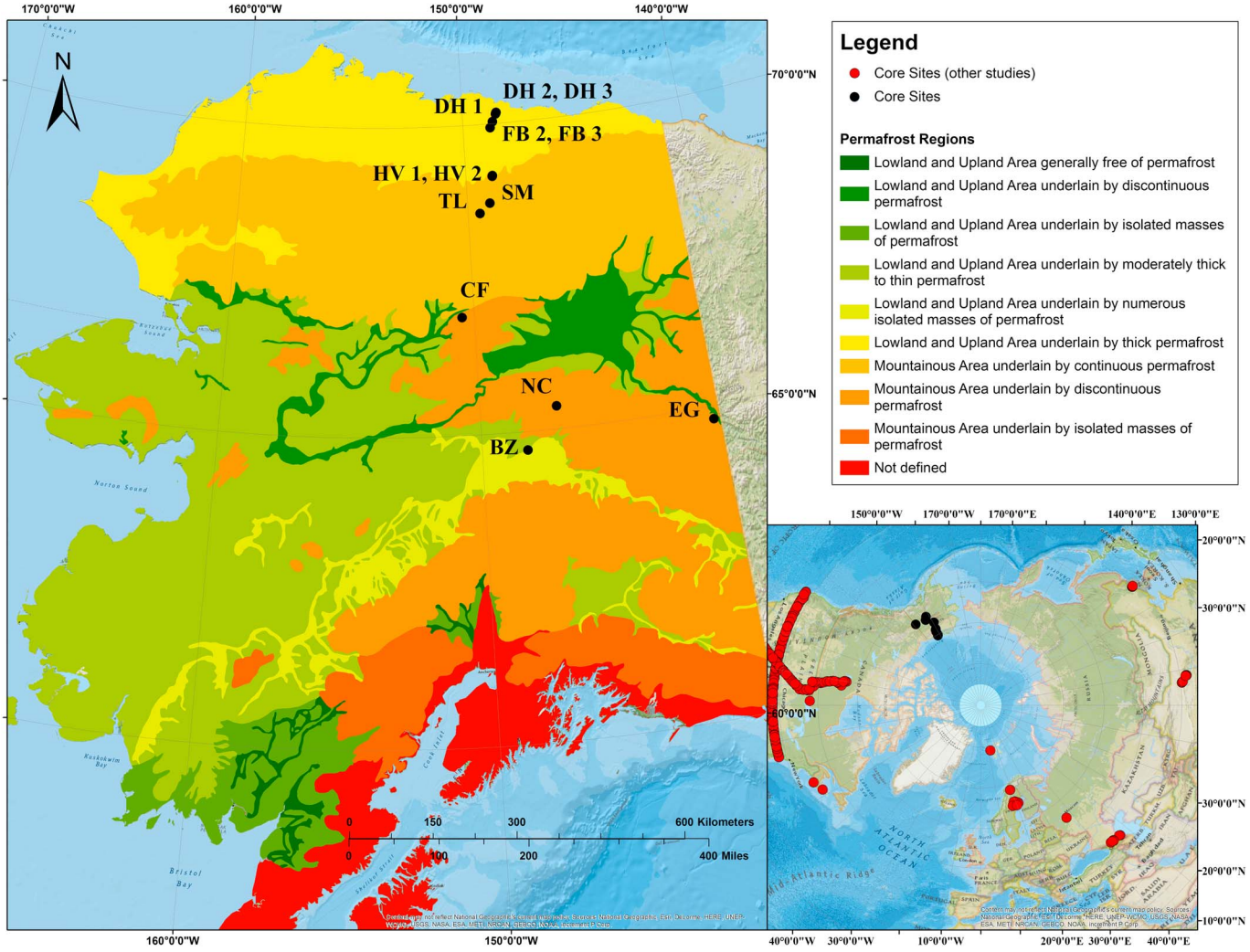

Figure 1. Locations of permafrost coring sites (black circles) and sites from other published studies (red circles) superimposed on a map of permafrost regions.

2. Site Descriptions and Methods

To estimate Hg in permafrost regions, we drilled 13 permafrost soil cores of variable lengths in Alaska along a ~500 km north-south transect representing a broad array of characteristics and ages typical of circumpolar permafrost soils (Figures 1 and S2–S10 and Tables S1 and S2). The maximum depths varied between 98 and 248 cm below the land surface, and the sites reflect a variety of depositional conditions. For each core we dug a pit down to the top of the permafrost and measured active layer depth (ALD). We extracted the cores using a gas-powered Snow, Ice, and Permafrost Research Establishment (SIPRE) auger modified with carbide cutting blades for frozen soil (Figure S11). The SIPRE can drill to a maximum depth of ~2 m, but obstructing rocks typically limited the actual drilling depth at each site. We broke each core into smaller samples, which we photographed, wrapped, labeled, and stored in a portable freezer (Figure S12). We shipped the frozen cores to the U.S. Geological Survey (USGS) Research Laboratory in Boulder, Colorado and stored them at −20°C until cutting, processing, and analysis.

We cut the cores in half lengthwise using a band saw thoroughly cleaned with methanol and 18 MegaOhm deionized water and archived one half in airtight bags in a freezer for future analyses (Figures S13 and S14). We then sliced the frozen cores into 1.5 cm segments for a total of 588 samples (Figure S15). We followed standard techniques of trace metal sampling with laboratory technicians wearing Latex gloves at all times (U.S. Geological Survey, 2015). Using a ceramic knife on a Teflon surface, we cut each frozen segment into

two rectangular subsamples from the center of the segment, one for STHg and one for bulk density (BD). We scraped off the outer few millimeters of the Hg subsample with the knife before measuring STHg (Figure S16). We weighed and measured the dimensions of the larger subsample to determine BD (Soil Survey Staff, 2014). We placed the STHg subsample in a preweighed, Hg-free jar, recorded the mass, and freeze-dried it (Figure S17). We thoroughly cleaned a mortar and pestle with 18 MegaOhm deionized water, homogenized the Hg subsample to a fine powder, and stored the powder in Hg-free glass vials (Figure S18).

We measured STHg, BD, soil organic carbon (SOC), and Δ14C and calculated the Hg to carbon ratio (R_{HgC}) (Table S3). Quality Assurance and Control accounted for more than 56% of all analyses (Texts S1–S3). We split every tenth segment into duplicate subsamples (Figure S19). For the CF and EG cores, we analyzed STHg at the USGS Mercury Research lab in Madison, Wisconsin using EPA Method 7473 (EPA Method 7473 (SW-846), 1998; USGS Mercury Research Lab (MRL), http://wi.water.usgs.gov/mercury-lab/analysis-methods.html, 2013). For all other cores, we measured STHg using a Milestone Direct Mercury Analyzer-80 (DMA-80) at the USGS Research Laboratory in Boulder, Colorado (Figure S20, Text S4, and Table S4). For soil carbon dating, we give $\Delta^{14}C$ concentration as the fraction Modern $\Delta^{14}C$ and conventional radiocarbon age (Text S5). We measured loss on ignition (LOI) for the second subsample as the loss of weight of a dried sample ignited at 550°C for 5 h by a Muffle furnace (Soil Survey Staff, 2014). To estimate SOC, we multiplied LOI by a carbon fraction of 0.493 (Anderson & Sarmiento, 1994). We used the standard Redfield ratio of 0.493 based on the 117:14:1 C;N;P; ratio of marine biomass samples. We calculated R_{HgC} as the ratio of STHg to SOC for each sample (Bargagli et al., 2007).

To create maps of soil Hg, we multiplied maps of soil carbon by a representative R_{HgC}. We used soil carbon maps from the Northern Circumpolar Soil Carbon Database (NCSCD) at a spatial resolution of 0.5° latitude and longitude (Hugelius, Tarnocai, et al., 2013; Hugelius et al., 2014). We calculated separate Hg maps for several soil layers: 0–30 cm, 0–60 cm 0–100 cm, 0–300 cm, active layer, and permafrost. We assume 300 cm represents the typical soil accumulation since the last glacial maximum to capture 90% of the carbon in the near surface soils. The active layer Hg extends from the surface to ALD, and the permafrost Hg extends from the ALD to 300 cm. We used simulated ALD from the Community Land Model version 3.4 (Koven et al., 2015) and a linear fit of cumulative SOC with depth from the profiles in Harden et al. (2012). We ignore localized deposits in yedoma and deltaic soils known to extend below 300 cm. We account for the fact that permafrost occurs only under 50–90% of the land area in discontinuous zones and for the volume of soil taken up by excess ground ice (Hugelius, Tarnocai, et al., 2013; Hugelius et al., 2014).

We used the median as the representative R_{HgC} with uncertainty as the 25th to 75th percentiles. We use quadrature to combine uncertainty of R_{HgC} with the 14.5% uncertainty in soil carbon from the NCSCD. We statistically evaluated the representativeness of the median R_{HgC} by subdividing the data and determining if the median R_{HgC} changes between sites, depths, and soil types. We regressed R_{HgC} against ^{14}C age to evaluate the representativeness of the median R_{HgC} over time. We evaluated the spatial representativeness of our measurements by comparison with 11,000 published measurements. Less than 2% of published data come from permafrost sites, so we included data from boreal and temperate sites (Table S5 and S6). We included only sites with both SOC and STHg measurements to calculate R_{HgC}. The published data included extreme outliers indicative of modern Hg contamination that biased the statistics. Our samples stayed frozen for thousands of years and represent preindustrial conditions, so to make a fair comparison, we removed outliers exceeding the mean plus 2 times the standard deviation (73 STHg and 125 R_{HgC} values). This resulted in 11,000 published measurements of STHg, SOC, and R_{HgC} from 4,926 different sites.

3. Results

We find a median STHg of 43 ± 30 ng Hg g $soil^{-1}$ and a median representative R_{HgC} of 1.6 ± 0.9 μg Hg g C^{-1} (Figure 2). For both STHg and R_{HgC}, the median and mean values for our data match each other and those from the published data within uncertainty. The published data show a higher mean R_{HgC} because it has 11% or ~1,100 STHg values greater than 200 ng Hg g $soil^{-1}$, compared to one sample in our data, indicating local contamination by anthropogenic sources at some sites. Our STHg data showed a bimodal distribution with a primary peak at 40 ng Hg g $soil^{-1}$ and a weaker secondary peak at 100 ng Hg g $soil^{-1}$ resulting from data from four of the cores, indicating strong variability between sites. The published data also show

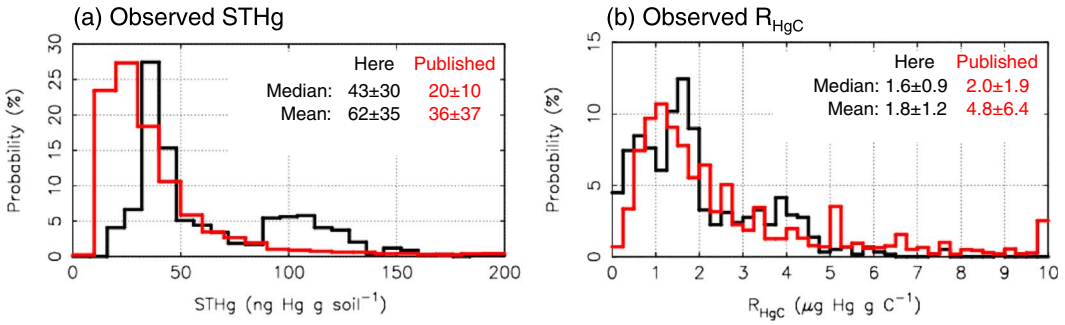

Figure 2. Probability functions showing the fraction of values as a function of (a) STHg and (b) R_{HgC}. Our data for permafrost soils appear in black, and published data for mostly nonpermafrost soils appear in red.

variability between sites, but the secondary peak does not appear at all. Our data and the published data both show a single dominant mode in R_{HgC}, with 95.5% of the R_{HgC} values falling between 0.0 and 5.0 μg Hg g C^{-1}.

The median R_{HgC} of 1.6 ± 0.9 μg Hg g C^{-1} appears representative of site, depth, soil type, and age. STHg showed high variability between sites, but the median R_{HgC} is insensitive to site (Figure S21). Comparing our sites to maps of soil characteristics indicates the cores broadly represent ~69% of the soils found in Alaska (Hugelius, Tarnocai, et al., 2013; Hugelius et al., 2014). R_{HgC} does not change with soil type: mineral and peat soils have roughly the same median R_{HgC}. Although STHg and SOC both decrease with depth (Figures S22 and S23), R_{HgC} is constant with depth: the R_{HgC} median for any 20 cm range of depths is 1.6 μg Hg g C^{-1} (Figures S24 and S25). Because age decreases exponentially with depth, SOC and STHg also decrease with age. However, unlike STHg and SOC, R_{HgC}, appears constant with age (Figures S26–S29).

Maps of soil Hg show great spatial variability reflecting different sedimentation histories (Figure 3). The relative uncertainty per pixel is 57%, which means there is a 95% probability that the actual value lies within ±57% of our estimated value. Soils with high carbon content and high sedimentation show high Hg mass, such as the North Slope of Alaska and the Mackenzie River basin in Canada. Areas with little sedimentary overburden and shallow soils such as the Rocky Mountains and the Canadian Shield in North America have low SOC and Hg. Slow decay due to freezing temperatures coupled with high sedimentation rates has buried substantial amounts of carbon and Hg over much of Siberia. The active layer depth (ALD) varies from 30 cm near the Arctic coastline to 100 cm in the southern permafrost regions, so much of the buried carbon and the Hg bound to it lies frozen and preserved in permafrost. Our 0–30 cm map agrees with a published 0–30 soil Hg map in areas with little sedimentary overburden but shows much higher soil Hg in areas with high sedimentation rates, particularly Siberia (Smith-Downey et al., 2010). A large pool of Hg in the active layer leaching into Arctic Rivers might explain why the permafrost-dominated terrestrial environment is the dominant source of Hg to the Arctic Ocean and why the Arctic Ocean is a net source of Hg to the Atlantic and Pacific Oceans (Fisher et al., 2012; Schuster et al., 2011; Soerensen et al., 2016).

4. Discussion

Several atmospheric Hg sources unique to the northern high latitudes have significant spatial and temporal variability to explain STHg variability within and between cores (Fitzgerald & Lamborg, 2003). Northern boreal forest fires release Hg into the atmosphere leading to spatial variability in Hg deposition (Homann et al., 2015; Rothenberg et al., 2010; Turetsky, et al., 2006). Spatial variations in temperature and moisture change microbial respiration rates (Wickland et al., 2006). Peaks in atmospheric Hg during summer resulting from atmospheric mixing with ozone enhance Hg deposition (Banic et al., 2003; Sonke & Heimbürger, 2012). Springtime atmospheric Hg depletion after the polar sunrise may elevate Hg deposition to the high latitudes (Berg et al., 2008; Fitzgerald et al., 2005; Lindberg et al., 2002). Although southeast Alaska contains geologic Hg deposits (Gray et al., 2000), we see no evidence of terrestrial geologic Hg sources within Alaska (Eberl, 2004; Williams, 1962). Volcanic eruptions release Hg into the atmosphere, leading to variability in Hg deposition (Pirrone et al., 2010; Pyle & Mather, 2003; Schuster et al., 2002), but we saw little evidence of Hg

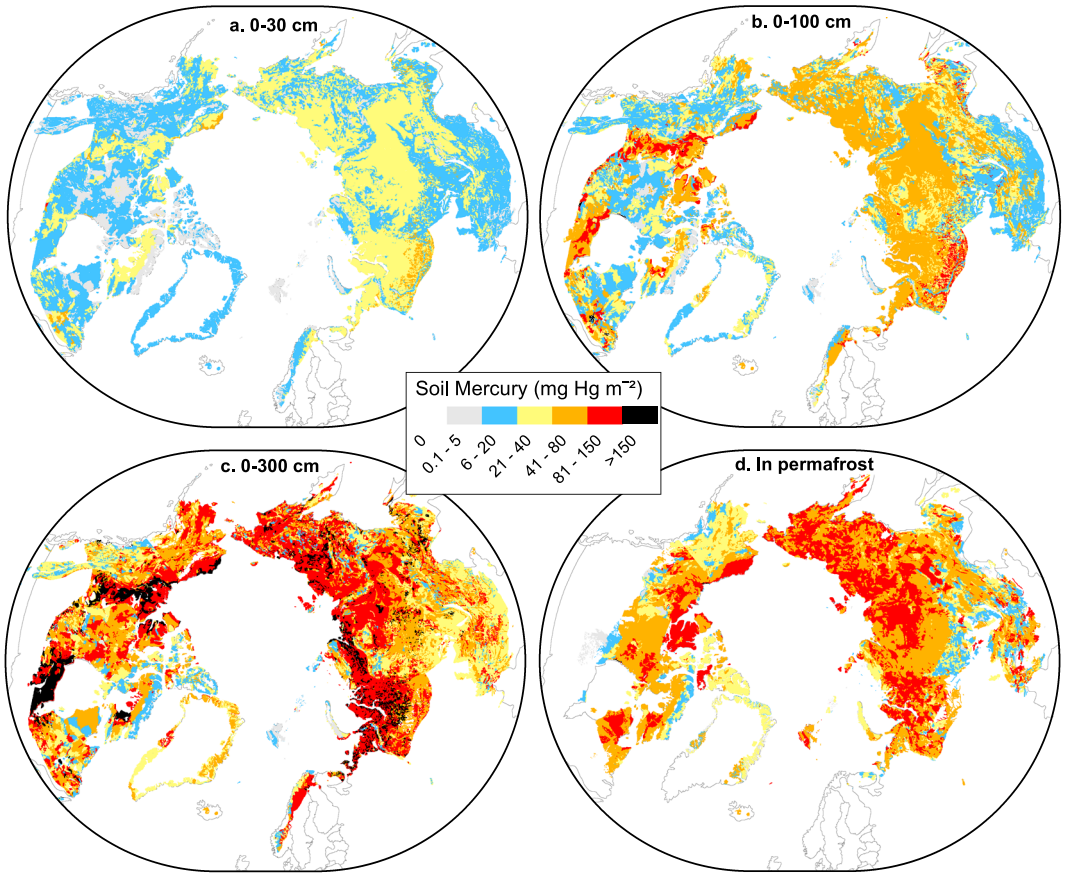

Figure 3. Maps of Hg (mg Hg m^{-2}) in Northern Hemisphere permafrost zones for four soil layers: 0–30 cm, 0–100 cm, 0–300 cm, and permafrost derived by multiplying maps of carbon from Hugelius, Tarnocai, et al. (2013) and Hugelius et al. (2014) by the median R_{HgC}. The permafrost map represents the Hg bound to frozen organic matter below the ALD and above 300 cm depth. The relative uncertainty is 57% for all pixels.

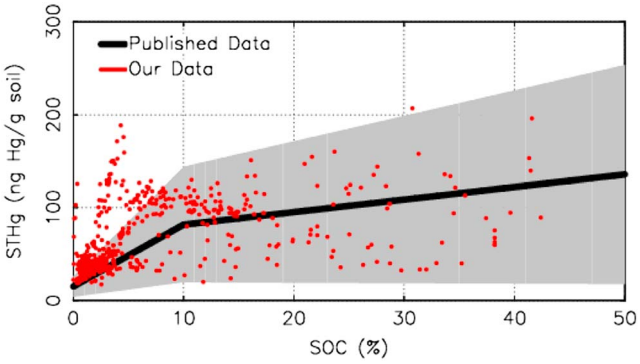

Figure 4. STHg as a function of SOC for our data (red dots), the median of the published data (black line), and the 90% envelope of published data (grey areas). For SOC < 10%, the median STHg for the published data increases linearly with an R^2 of 0.98. For SOC > 10%, the slope of the median STHg drops and the relationship weakens with an R^2 of 0.56. About 90% of our data values fall within the expected envelope of the published data (Figures S30–S32).

deposition from volcanic ash. These depositional processes are not exclusive to the 13 coring sites chosen for this study but rather inclusive to the high latitudes of the Northern Hemisphere.

Despite these processes leading to highly variable depositional environments, our STHg measurements appear consistent with similar measurements in permafrost regions. Peat deposits in Tomsk Oblast, west Siberia (Lyapina et al., 2009) show STHg values and vertical profiles similar to ours. Rydberg et al. (2010) measured STHg of 40 ng Hg g $soil^{-1}$ below 25 cm depth, close to our median value of 43 ng Hg g $soil^{-1}$. STHg in active layer soils along a ~970 kilometer north-south transect of Alaska ranged from 100 ng Hg g $soil^{-1}$ in the O horizon to 50 ng Hg g $soil^{-1}$ in the A horizon (Wang et al., 2010). STHg ranged between 12 and 375 ng Hg g $soil^{-1}$, and R_{HgC} varied between 1 and 11.3 μg Hg g C^{-1} at a sub-Antarctic site in Tierra del Fuego (Peña-Rodríguez et al., 2014).

Moreover, our STHg measurements appear consistent with published data for nonpermafrost soils (Figure 4). Most of the 11,000 published data fall in the temperate midlatitudes, with 2088 in boreal forests and only 67 points in permafrost regions. Here we show a curve fit of the median STHg as a function of SOC with the 90% envelope defined as the 5th to 95th percentiles (Figures S30–S32). Superimposing our data

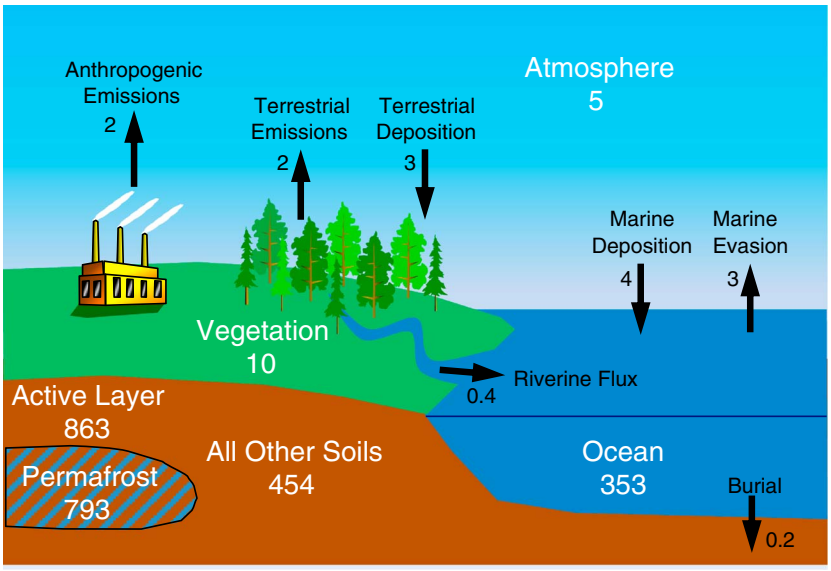

Figure 5. An updated schematic of the modern global Hg cycle with major reservoirs in white (Gg Hg) and fluxes in black (Gg Hg yr^{-1}). Adapted from Amos et al. (2013) with the soil reservoir shown as an average of previously published estimates (Table S7).

indicates that 90% of our STHg measurements fall within the 90% envelope of the published data, with a slight shift toward higher STHg.

As SOC increases, STHg appears to shift from a receptor-limited regime to a flux-limited regime (Figure 4). Hg enters plants through the roots or by dry deposition from the atmosphere onto leaves (Obrist et al., 2017; Windham-Myers et al., 2009), where it attaches to appropriate receptor sites in organic molecules in place of nutrients such as iron or magnesium. For mineral soils with SOC $<$ 10%, the number of receptor sites limit the Hg plants can retain, and STHg increases strongly with SOC (R^2 = 0.98). For organic soils with SOC $>$ 10%, receptor sites appear unlimited and the flux of Hg from the atmosphere limits the STHg. Since atmospheric deposition is highly variable in space and time, the data become noisier and STHg appears nearly independent of SOC. The two regimes might explain why, like previously published data (Bargagli et al., 2007; Erickson, 2014), some sites show statistically significant correlations between STHg and SOC, whereas others did not. Sites with low SOC in the receptor-limited regime tended to have statistically significant correlations, while sites with organic soils in the flux-limited regime did not.

We estimate that soils in permafrost regions contain an estimated 1,656 ± 962 Gg Hg, of which half or 793 ± 461 Gg Hg is frozen in permafrost (Figure 5 and Table 1). We estimate the total mass of Hg in each layer by multiplying each pixel by the grid cell area and summing across the permafrost domain. The average of nine previously published estimates of global soil Hg is 454 ± 321, with a range from 235 to 1,000 Gg Hg (Table S7). However, these estimates generally limit soil depth to 30 cm, indicating our 0–30 cm soil Hg for permafrost regions (347 ± 196 Gg Hg; Table 1) rivals the global soil Hg in previous estimates. These studies leverage the known link between microbial decay and Hg release and often rely on biogeochemical models that tend to underestimate soil Hg in permafrost regions. To improve Hg estimates in permafrost soils, these models should account for the large drop in microbial activity under freezing conditions and sedimentation processes that bury and freeze organic matter into the permafrost. Our results indicate the active layer alone represents the largest Hg reservoir on the planet. The active layer and permafrost together contain nearly twice as much Hg as all other soils, the ocean, and the atmosphere combined.

Table 1
Total Soil Carbon and Hg in Northern Hemisphere Permafrost Regions

Depth range (cm)	Soil carbon (Pg)	Soil Hg (Gg Hg)
0–30	217 ± 12	347 ± 196
0–60	333 ± 18	532 ± 301
0–100	472 ± 27	755 ± 427
0–200	827 ± 108	1323 ± 764
0–300	1035 ± 150	1656 ± 962
Permafrost	496 ± 72	793 ± 461
Active layer	539 ± 78	863 ± 501

Hg in permafrost soils represents an environmental risk as permafrost continues to thaw in the future. The turnover time associated with the

microbial decay of frozen organic matter is ~14,000 years (Figure S28), making the Hg locked in permafrost effectively stable on human time scales. However, projections indicate a 30–99% reduction in near surface permafrost by 2100, and, once thawed, the turnover time for microbial decay drops to ~70 years (Koven et al., 2013; Schaefer et al., 2011). This makes the reservoir of Hg in permafrost soils vulnerable to release over the next century, with unknown consequences to the environment.

5. Summary

We measured a median STHg of 43 ± 30 ng Hg g soil^{-1} and a median R_{HgC} of 1.6 ± 0.9 μg Hg g C^{-1} based on 588 samples from 13 soil permafrost cores from the interior and the North Slope of Alaska. These values appear consistent with published results of Hg concentrations for tundra soils and 11,000 nonpermafrost soil measurements from 4,926 different sites in North America and Eurasia. In a novel approach, we estimate that the entire Northern Hemisphere permafrost region contains 1,656 ± 962 Gg Hg, of which 793 ± 461 Gg Hg is frozen in permafrost. Northern Hemisphere permafrost soils contain nearly twice as much Hg as all other soils, the ocean, and the atmosphere combined, indicating a need to reevaluate the role of the Arctic regions in the global Hg cycle. This Hg is vulnerable to release as permafrost thaws over the next century.

Any use of trade, firm, or product names is for descriptive purposes only and does not imply endorsement by the U.S. Government.

Acknowledgments
The authors thank John Borg, John Crawford, and Bob Eaganhouse for drilling assistance. This article is dedicated to George R. Aiken, whose 40 year career as a U.S. Geological Survey scientist was cut short with his death from cancer in 2016. Without George's foundational scientific contributions to our knowledge of the world's organic matter, much of what we know about organic matter would not have been possible, including the findings from this study. George is missed by too many friends and family to count. However, his legacy as "Dr DOC" will live on in all of us. Supporting Information (SI) are available at http://agupubs.onlinelibrary.wiley.com/hub/journal/10.1002/(ISSN)1944-8007/. Data generated for this study are available at https://www.sciencebase.gov/catalog/ domain repository and GeoPass: https://geopass.iedadata.org/josso/. Reprints and permission information are available at https://grl-submit.agu.org/. The authors declare no competing financial interests. Readers are welcome to comment on the online version of this paper. Correspondence and request for materials should be addressed to pschuste@usgs.gov (https://orcid.org/0000-0002-8314-1372) or kevin.schaefer@nsidc.org. Funding for this research came from the USGS Toxic Substances Hydrology Program (TSHP) and the USGS NASQAN/NAWQA and CEN Programs; NASA grants NNX10AR63G, NNX06AE65G, NNX17AC59A, and NNX13AM25G; NOAA grant NA09OAR4310063; CUHK Direct grant 4053206; the National Natural Science Foundation of China (91325202); the National Key Scientific Research Project (2013CBA01802) by the Ministry of Science and Technology of China; and National Science Foundation grant ARC1204167. G.H. received funding from the EU H2020 Nunataryuk project (773421). P. S. devised and supervised the study, drilled four cores, and supervised all laboratory work. K. M. S. supervised the collection of the other cores and analyzed data. D. P. K., R. G. S., K. P. W., and G. R. A. provided advice and guidance during writing. R. C. A. provided statistical support. J. F. D. analyzed and quality assured data from two cores. J. D. G. and C. W. processed all the cores. G. H. led map development. E. J. assisted with the writing process and references. N. H. M. contributed to map development. A. G., E. J., L. L., T. S., and T. Z. drilled one or more cores. D. A. R. wrote the standard operation procedure for the DMA-80, maintained the instrument, and processed and quality assured 85% of the data.

References

Amos, H. M., Jacob, D. J., Kocman, D., Horowitz, H. M., Zhang, Y., Dutkiewicz, S., … Sunderland, E. M. (2014). Global biogeochemical implications of mercury discharges from rivers and sediment burial. *Environmental Science & Technology*, *48*(16), 9514–9522. https://doi.org/10.1021/es502134t

Amos, H. M., Jacob, D. J., Streets, D. G., & Sunderland, E. M. (2013). Legacy impacts of all-time anthropogenic emissions on the global mercury cycle. *Global Biogeochemical Cycles*, *27*, 410–421. https://doi.org/10.1002/gbc.20040

Amos, H. M., Sonke, J. E., Obrist, D., Robins, N., Hagan, N., Horowitz, H. M., … Sunderland, E. M. (2015). Observational and modeling constraints on global anthropogenic enrichment of mercury. *Environmental Science & Technology*, *49*(7), 4036–4047. https://doi.org/10.1021/es5058665

Anderson, L. A., & Sarmiento, J. L. (1994). Redfield ratios of remineralization determined by nutrient data analysis. *Global Biogeochemical Cycles*, *8*(1), 65–80. https://doi.org/10.1029/93GB03318

Banic, C. M., Beauchamp, S. T., Tordon, R. J., Schroeder, W. H., Steffen, A., Anlauf, K. A., & Wong, H. K. T. (2003). Vertical distribution of gaseous elemental mercury in Canada. *Journal of Geophysical Research*, *108*(D9), 4264. https://doi.org/10.1029/2002JD002116

Bargagli, R., Monaci, F., & Bucci, C. (2007). Environmental biogeochemistry of mercury in Antarctic ecosystems. *Soil Biology & Biochemistry*, *39*(1), 352–360. https://doi.org/10.1016/j.soilbio.2006.08.005

Berg, T., Aspmo, K., & Steinnes, E. (2008). Transport of Hg from atmospheric mercury depletion events to the mainland of Norway and its possible influence on Hg deposition. *Geophysical Research Letters*, *35*, L09802. https://doi.org/10.1029/2008GL033586

Dunlap, K. L., Reynolds, A. J., Bowers, P. M., & Duffy, L. K. (2007). Hair analysis in sled dogs (*Canis lupus familiaris*) illustrates a linkage of mercury exposure along the Yukon River with human subsistence food systems. *Science of the Total Environment*, *385*(1-3), 80–85. https://doi.org/10.1016/j.scitotenv.2007.07.002

Eberl, D. D. (2004). Quantitative mineralogy of the Yukon River system: Variations with reach and season, and sediment source unmixing. *American Mineralogist*, *89*(11-12), 1784–1794. https://doi.org/10.2138/am-2004-11-1225

EPA Method 7473 (SW-846) (1998). Mercury in solids and solutions by thermal decomposition, amalgamation, and atomic absorption spectrophotometry, Revision 0.

Erickson, L. (2014). Mercury dynamics in sub-arctic lake sediments across a methane ebullition gradient, Thesis, Geology Gustavus Adolphus College, pp. 30.

Fisher, J. A., Jacob, D. J., Soerensen, A. L., Amos, H. M., Steffen, A., & Sunderland, E. M. (2012). Riverine source of Arctic Ocean mercury inferred from atmospheric observations. *Nature Geoscience*, *5*(7), 499–504. https://doi.org/10.1038/NGEO1478

Fitzgerald, W. F., Engstrom, D. R., Lamborg, Tseng, C.-M., Balcom, P. H., & Hammerschmidt, C. R. (2005). Modern and historic atmospheric mercury fluxes in northern Alaska: Global sources and Arctic depletion. *Environmental Science & Technology*, *39*(2), 557–568. https://doi.org/10.1021/es049128x

Fitzgerald, W. F., & Lamborg, C. H. (2003). Geochemistry of mercury in the environment. In H. D. Holland, & K. K. Turekian (Eds.), *Treatise on geochemistry* (Vol. 9, pp. 107–148). Amsterdam: Elsevier. https://doi.org/10.1016/B0-08-043751-6/09048%E2%80%934

Gallant, A. L., Whittier, T. R., Larsen, D. P., Omernik, J. M., & Hughes, R. M. (1989). Regionalization as a tool for managing environmental resources. EPA/600/3–89/060. US Environmental Protection Agency, Environmental Research Laboratory, Corvallis, Oregon, 152 pp.

Gray, J. E., Theodorakos, P. M., Bailey, E. A., & Turner, R. R. (2000). Distribution, speciation, and transport of mercury instream-sediment, stream-water, and fish collected near abandoned mercury mines in southwestern Alaska, USA. *The Science of the Total Environment*, *260*(1-3), 21–33. https://doi.org/10.1016/S0048-9697(00)00539-8

Hararuk, O., Obrist, D., & Luo, Y. (2013). Modelling the sensitivity of soil mercury storage to climate-induced changes in soil carbon pools. *Biogeosciences*, *10*(4), 2393–2407. https://doi.org/10.5194/bg-10-2393-2013

Harden, J. W., Koven, C. D., Ping, C. L., Hugelius, G., McGuire, A. D., Camill, P., … Grosse, G. (2012). Field information links permafrost carbon to physical vulnerabilities of thawing. *Geophysical Research Letters*, *39*, L15704. https://doi.org/10.1029/2012GL051958

Hinzman, L. D., Bettez, N. D., Bolton, W. R., Chapin, F. S., Dyurgerov, M. B., Fastie, C. L., … Yoshikawa, K. (2005). Evidence and implications of recent climate change in northern Alaska and other Arctic regions. *Climatic Change*, *72*(3), 251–298. https://doi.org/10.1007/s10584-005-5352-2

Holmes, C. D., Jacob, D. J., Corbitt, E. S., Mao1, J., Yang, X., Talbot, R., & Slemr, F. (2010). Global atmospheric model for mercury including oxidation by bromine atoms. *Atmospheric Chemistry and Physics*, *10*(24), 12,037–12,057. https://doi.org/10.5194/acp-10-12037-2010

Homann, P. S., Garbyshire, R. L., Bormann, B. T., & Morrissette, B. A. (2015). Forest structure affects soil mercury losses in the presence and absence of wildfire. *Environmental Science & Technology*, *49*(21), 12,714–12,722. https://doi.org/10.1021/acs.est.5b03355

Hugelius, G., Bockheim, J. G., Camill, P., Elberling, B., Grosse, G., Harden, J. W., … Yu, Z. (2013). A new data set for estimating organic carbon storage to 3 m depth in soils of the northern circumpolar permafrost region. *Earth System Science Data*, *5*(2), 393–402. https://doi.org/10.5194/essd-5-393-2013

Hugelius, G., Strauss, J., Zubrzycki, S., Harden, J. W., Schuur, E. A. G., Ping, C. L., … Kuhry, P. (2014). Estimated stocks of circumpolar permafrost carbon with quantified uncertainty ranges and identified data gaps. *Biogeosciences*, *11*(23), 6573–6593. https://doi.org/10.5194/bg-11-6573-2014

Hugelius, G., Tarnocai, C., Broll, G., Canadell, J. G., Kuhry, P., & Swanson, D. K. (2013). The northern circumpolar soil carbon database: Spatially distributed datasets of soil coverage and soil carbon storage in the northern permafrost regions. *Earth System Science Data*, *5*, 3–13. https://doi.org/10.5194/essd-5-3-2013

Jiang, S., Liu, X., & Chen, Q. (2011). Distribution of total mercury and methylmercury in lake sediments in Arctic Ny-Ålesund. *Chemosphere*, *83*(8), 1108–1116. https://doi.org/10.1016/j.chemosphere.2011.01.031

Jonsson, S., Andersson, A., Nilsson, M. B., Skyllberg, U., Lundberg, E., Schaefer, J. K., … Björn, E. (2017). Terrestrial discharges mediate trophic shifts and enhance methylmercury accumulation in estuarine biota. *Science Advances*, *3*(1), e1601239. https://doi.org/10.1126/sciadv.1601239

Kang, S., Huang, J., Wang, F., Zhang, Q., Zhang, Y., Li, C., … Guo, J. Atmospheric mercury depositional chronology reconstructed from lake sediments and ice core in the Himalayas and Tibetan Plateau. *Environmental Science & Technology*, *50*(6), 2859–2869. https://doi.org/10.1021/acs.est.5b04172

Klaminder, J., Bindler, R., Rydberg, J., & Renberg, I. (2008). Is there a chronological record of atmospheric mercury and lead deposition preserved in the mor layer (O-horizon) of boreal forest soils? *Geochimica et Cosmochimica Acta*, *72*(3), 703–712. https://doi.org/10.1016/j.gca.2007.10.030

Kolka, R. K., Sturtevant, B. R., Miesel, J. R., Singh, A., Wolter, P. T., Fraver, S., … Townsend, P. A. (2017). Emissions of forest floor and mineral soil carbon, nitrogen and mercury pools and relationships with fire severity for the Pagami Creek fire in the boreal forest of northern Minnesota. *International Journal of Wildland Fire*, *26*(4), 296–305. https://doi.org/10.1071/WF16128

Koven, C. D., Riley, W. J., & Stern, A. (2013). Analysis of permafrost thermal dynamics and response to climate change in the CMIP5 Earth system models. *Journal of Climate*, *26*(6), 1877–1900. https://doi.org/10.1175/JCLI-D-12-00228.1

Lindberg, S. E., Brooks, S., Lin, C. J., Scott, K. J., Landis, M. S., Stevens, R. K., … Richter, A. (2002). Mercury in the Arctic troposphere at polar sunrise. *Environmental Science & Technology*, *36*(6), 1245–1256. https://doi.org/10.1021/es0111941

Lindqvist, O., Johansson, K., Aastrup, M., Andersson, A., Bringmark, L., Hovsenius, G., … Timm, B. (1991). Mercury in the Swedish environment—Recent research on causes, consequences and corrective methods. *Water, Air, and Soil Pollution*, *55*, 11–13.

Lyapina, E. E., Golovatskaya, E. A., & Ippolitov, I. I. (2009). Mercury concentration in natural objects of West Siberia. *Contemporary Problems of Ecology*, *2*(1), 1–5. https://doi.org/10.1134/S1995425509010019

Mason, R. P., Choi, A. L., Fitzgerald, W. F., Hammerschmidt, C. R., Lamborg, C. H., Soerensen, A. L., & Sunderland, E. M. (2012). Mercury biogeochemical cycling in the ocean and policy implications. *Environmental Research*, *119*, 101–117. https://doi.org/10.1016/j.envres.2012.03.013

Obrist, D., Agnan, Y., Jiskra, M., Olson, C. L., Colegrove, D. P., Hueber, J., … Helmig, D. (2017). Tundra uptake of atmospheric elemental mercury drives Arctic mercury pollution. *Nature*, *547*(7662), 201–204. https://doi.org/10.1038/nature22997

Pannu, R., Siciliano, S. D., & O'Driscoll, N. J. (2014). Quantifying the effects of soil temperature, moisture and sterilization on elemental mercury formation in boreal soils. *Environmental Pollution*, *193*, 138–146. https://doi.org/10.1016/j.envpol.2014.06.023

Peña-Rodríguez, S., Pontevedra-Pombal, X., Gayoso, E. G. R., Moretto, A., Mansilla, R., Cutillas-Barreiro, L., … Nóvoa-Muñoz, J. C. (2014). Mercury distribution in a toposequence of sub-Antarctic forest soils of Tierra del 2 Fuego (Argentina) as consequence of the prevailing soil processes. *Geoderma*, *232-234*, 130–140. https://doi.org/10.1016/j.geoderma.2014.04.040

Pirrone, N., Cinnirella, S., Feng, X., Finkelman, R. B., Friedli, H. R., Leaner, J., … Telmer, K. (2010). Global mercury emissions to the atmosphere from anthropogenic and natural sources. *Atmospheric Chemistry and Physics*, *10*(13), 5951–5964. https://doi.org/10.5194/acp-10-5951-2010

Podar, M., Gilmour, C., Brandt, C. C., Soren, A., Brown, S. D., Crable, B. R., … Elias, D. A. (2015). Global prevalence and distribution of genes and microorganisms involved in mercury methylation. *Science Advances*, *1*(9), e1500675–e1500612. https://doi.org/10.1126/sciadv.1500675.

Pyle, D. M., & Mather, T. A. (2003). The importance of volcanic emissions for the global atmospheric mercury cycle. *Atmospheric Environment*, *37*(36), 5115–5124. https://doi.org/10.1016/j.atmosenv.2003.07.011

Romanovsky, V., Grosse, G., & Marchenko, S. (2008). Past, present and future of permafrost in a changing world. *Geological Society of America*, *40*(6), 397.

Rothenberg, S. E., Kirby, M. E., Bird, B. W., DeRose, M. B., Lin, C. C., Feng, X., … Jay, J. A. (2010). The impact of over 100 years of wildfires on mercury levels and accumulation rates in two lakes in southern California, USA. *Environment and Earth Science*, *60*(5), 993–1005. https://doi.org/10.1007/s12665-009-0238-7

Rydberg, J., Klaminder, J., Rosén, P., & Bindler, R. (2010). Climate driven release of carbon and mercury from permafrost mires increases mercury loading to sub-arctic lakes. *Science of the Total Environment*, *408*(20), 4778–4783. https://doi.org/10.1016/j.scitotenv.2010.06.056

Schaefer, K., & Jafarov, E. (2016). A parameterization of respiration in frozen soils based on substrate availability. *Biogeosciences*, *13*(7), 1991–2001. https://doi.org/10.5194/bg-13-1991-2016

Schaefer, K., Lantuit, H., Romanovsky, V. E., Schuur, E. A. G., & Witt, R. (2014). The impact of the permafrost carbon feedback on global climate. *Environmental Research Letters*, *9*(8), 085003. https://doi.org/10.1088/1748-9326/9/8/085003

Schuster, P. F., Krabbenhoft, D. P., Naftz, D. L., Cecil, L. D., Olson, M. L., DeWild, J. F., … Abbott, M. L. (2002). Atmospheric mercury deposition during the last 270 years: A glacial ice core record of natural and anthropogenic sources. *Environmental Science and Technology*, *36*(11), 2303–2310. https://doi.org/10.1021/es0157503

Schuster, P. F., Striegl, R. G., Aiken, G. R., Krabbenhoft, D. P., DeWild, J. F., Butler, K., … Dornblaser, M. (2011). Mercury export from the Yukon River basin and potential response to a changing climate. *Environmental Science and Technology*, *45*(21), 9262–9267. https://doi.org/10.1021/es202068b

Skogerboe, R. K., & Grant, C. L. (1970). Comments on the definition of the terms sensitivity and detection limit. *Spectroscopy Letters*, *3*(8-9), 215–220. https://doi.org/10.1080/00387017008081956

Skyllberg, U., Qian, J., Frech, W., Kang, X., & Bleam, W. F. (2003). Distribution of mercury, methyl mercury and organic sulphur species in soil, soil solution and stream of a boreal forest catchment. *Biogeochemistry*, *64*(1), 53–76. https://doi.org/10.1023/A:1024904502633

Smith, D. B., Cannon, W. F., Woodruff, L. G., Garrett, R. G., Klassen, R., Kilburn, J. E., … Jean, M. (2005). Major- and trace-element concentrations in soils from two continental-scale transects of the United States and Canada. U.S. Geological Survey Open-File Report 2005–1253, 20 p. Retrieved from http://pubs.usgs.gov/of/2005/1253/

Smith, D. B., Cannon, W. F., Woodruff, L. G., Solano, F., & Ellefsen, K. J. (2014). Geochemical and mineralogical maps for soils of the conterminous United States. U.S. Geological Survey Open-File Report 2014–1082, pp. 386. https://doi.org/10.3133/ofr20141082

Smith, S. L., Romanovsky, V. E., Lewkowicz, A. G., Burn, C. R., Mallard, M., Clow, G. D., … Throop, J. (2010). Thermal state of permafrost in North America: A contribution to the International Polar Year. *Permafrost and Periglacial Processes*, *21*(2), 117–135. https://doi.org/10.1002/ppp.690

Smith-Downey, N. V., Sunderland, E. M., & Jacob, D. J. (2010). Anthropogenic impacts on global storage and emissions of mercury from terrestrial soils: Insights from a new global model. *Journal of Geophysical Research*, *115*, G03008. https://doi.org/10.1029/2009JG001124

Soerensen, A. L., Jacob, D. J., Schartup, A. T., Fisher, J. A., Lehnherr, I., St. Louis, V. L., … Sunderland, E. M. (2016). A mass budget for mercury and methylmercury in the Arctic Ocean. *Global Biogeochemical Cycles*, *30*, 560–575. https://doi.org/10.1002/2015GB005280

Soil Survey Staff (2014). Kellogg soil survey laboratory methods manual. Soil Survey Investigations Report No. 42, Version 5.0. R. Burt and Soil Survey Staff (ed.). U.S. Department of Agriculture, Natural Resources Conservation Service.

Sonke, J. E., & Heimbürger, L. E. (2012). Mercury in flux. *Nature Geoscience*, *5*(7), 447–448. https://doi.org/10.1038/ngeo1508

Turetsky, M. R., Harden, J. W., Friedli, H. R., Flannigan, M., Payne, N., Crock, J., & Radke, L. (2006). Wildfires threaten mercury stocks in northern soils. *Geophysical Research Letters*, *33*, L16403. https://doi.org/10.1029/2005GL025595

U.S. Geological Survey (2015). National field manual for the collection of water-quality data. U.S. Geological Survey Techniques of Water-Resources Investigations, book 9, Chaps. A1-A10, variously dated. Retrieved from http://pubs.water.usgs.gov/twri9A. http://water.usgs.gov/owq/FieldManual/chapter4/html/Ch4_contents.html

Wang, B., Eberl, D., Gough, L., & Frohbieter, D. (2010). Mercury in soils along a N/S transect in Alaska. In P. Birkle, & I. Torres-Alvarado (Eds.), *Proceedings of the 13th international symposium on water-rock interaction*, Guanajuato, Mexico, 16–20 August 2010. Water–Rock Interaction. (pp. 311–314).

Wickland, K. P., Krabbenhoft, D. P., & Olund, S. (2006). Evidence for a link between soil respiration and mercury emission from organic soils, Eighth International Conference on Mercury as a Global Pollutant, August 6-11.

Williams, J. R. (1962). Geologic reconnaissance of the Yukon Flats district, Alaska. *Geological Survey Bulletin*, *1111-H*, 289–331.

Windham-Myers, L., Marvin-Dipasquale, M., Krabbenhoft, D. P., Agee, J. L., Cox, M. H., Heredia-Middleton, P., … Kakouros, E. (2009). Experimental removal of wetland emergent vegetation leads to decreased methylmercury production in surface sediment. *Journal of Geophysical Research*, *114*, G00C5. https://doi.org/10.1029/2008JG000815

Zhang, L., Qian, J. L., & Planas, D. (1995). Mercury concentration in tree rings of black spruce (*Picea mariana* Mill. B.S.P.) in boreal Quebec, Canada. *Water, Air, and Soil Pollution*, *81*(1-2), 163–173. https://doi.org/10.1007/BF00477263

Zyrin, N. G., Zvonarev, B. A., & Kim, N. (1978). Mercury in the brown forest soils of Dagestan and the northern Osetiya. *Moscow University Soil Science Bulletin*, *12*, 22–26.

Zyrin, N. G., Zvonarev, B. A., Sadovnikova, L. K., & Voronova, N. I. (1981). Distribution of mercury in soils of the north Ossetian Plains. *Soviet Soil Science*, *13*, 44–52.

Erratum

In the originally published version of this article, there was a error in Figure 3 and its legend: (μg Hg m^{-2}) incorrectly appeared in place of the correct expression (mg Hg m^{-2}). These errors have been corrected, and the present version may be considered the authoritative version of record.